arXiv:1601.07597v1 [cs.NI] 27 Jan 2016

Flow Control and Scheduling for Shared FIFO Queues over Wireless Networks

Shanyu Zhou
University of Illinois at Chicago
szhou45@uic.edu

Hulya Seferoglu
University of Illinois at Chicago
hulya@uic.edu

Erdem Koyuncu
University of California, Irvine
ekoyuncu@uci.edu

***Abstract*—We investigate the performance of First-In, First-Out (FIFO) queues over wireless networks. We characterize the stability region of a general scenario where an arbitrary number of FIFO queues, which are served by a wireless medium, are shared by an arbitrary number of flows. In general, the stability region of this system is non-convex. Thus, we develop a convex inner-bound on the stability region, which is provably tight in certain cases. The convexity of the inner bound allows us to develop a resource allocation scheme; dFC. Based on the structure of dFC, we develop a stochastic flow control and scheduling algorithm; qFC. We show that qFC achieves optimal operating point in the convex inner bound. Simulation results show that our algorithms significantly improve the throughput of wireless networks with FIFO queues, as compared to the well-known queue-based flow control and max-weight scheduling.**

I. Introduction

The recent growth in mobile and media-rich applications continuously increases the demand for wireless bandwidth, and puts a strain on wireless networks [1], [2]. This dramatic increase in demand poses a challenge for current wireless networks, and calls for new network control mechanisms that make better use of scarce wireless resources. Furthermore, most existing, especially low-cost, wireless devices have a relatively rigid architecture with limited processing power and energy storage capacities that are not compatible with the needs of existing theoretical network control algorithms. One important problem, and the focus of this paper, is that low-cost wireless interface cards are built using First-In, First-Out (FIFO) queueing structure, which is not compatible with the per-flow queueing requirements of the optimal network control schemes such as backpressure routing and sheduling [3].

The backpressure routing and scheduling paradigm has emerged from the pioneering work [3], [4], which showed that, in wireless networks where nodes route and schedule packets based on queue backlogs, one can stabilize the queues for any feasible traffic. It has also been shown that backpressure can be combined with flow control to provide utility-optimal operation [5]. Yet, backpressure routing and scheduling require each node in the network to construct per-flow queues. The following example demonstrates the operation of backpressure.

Example 1: Let us consider a canonical example in Fig. 1(a), where a transmitter node S, and two receiver nodes A, B form a one-hop downlink topology. There are two flows with arrival rates $\lambda_{S,A}$ and $\lambda_{S,B}$ destined to nodes A and B, respectively. The throughput optimal backpressure scheduling scheme, also known as max-weight scheduling, assumes the availability of per-flow queues $Q_{S,A}$ and $Q_{S,B}$ as

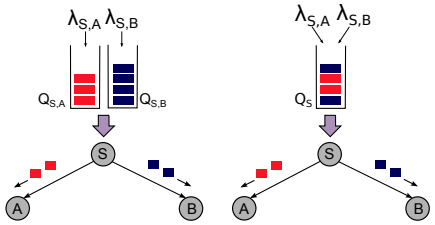

(a) Per-flow queues (b) FIFO queue

Fig. 1. Queueing structure of one-hop downlink topology with (a) per-flow queues, and (b) a FIFO queue.

seen in Fig. 1(a), and makes a transmission decision at each transmission opportunity based on queue backlogs, *i.e.*, $Q_{S,A}$ and $Q_{S,B}$. In particular, the max-weight scheduling algorithm determines $F^* = \arg\max_{F\in\{A,B\}} Q_{S,F}$, and transmits from queue Q_{S,F^*}. It was shown in [3], [4] that if the arrival rates $\lambda_{S,A}$ and $\lambda_{S,B}$ are inside the stability region of the wireless network, the max-weight scheduling algorithm stabilizes the queues. On the other hand, in some devices, per-flow queues cannot be constructed. In such a scenario, a FIFO queue, say Q_S is shared by flows A and B as shown in Fig. 1(b), and the packets are served from Q_S in a FIFO manner. □

Constructing per-flow queues may not be feasible in some devices especially at the link layer due to rigid architecture, and one FIFO queue is usually shared by multiple flows. For example, although current WiFi-based devices have more than one hardware queue [6], their numbers are restricted (up to 12 queues according to the list in [6]), while the number of flows passing through a wireless device could be significantly higher. Also, multiple queues in the wireless devices are mainly constructed for prioritized traffic such as voice, video, etc., which further limits their usage as per-flow queues. On the other hand, constructing per-flow queues may not be preferable in some other devices such as sensors or home appliances for which maintaining and handling per-flow queues could introduce too much processing and energy overhead. Thus, some devices, either due to rigid architecture or limited processing power and energy capacities, inevitably use shared FIFO queues, which makes the understanding of the behavior of FIFO queues over wireless networks very crucial.

Example 1 - continued: Let us consider Fig. 1 again. When a FIFO queue is used instead of per-flow queues, the well-known head-of-line (HOL) blocking phenomenon occurs. As an example, suppose that at transmission instant t, the links $S-A$ and $S-B$ are at "ON" and "OFF" states, respectively. In this case, a packet from $Q_{S,A}$ can be transmitted if per-

flow queues are constructed. Yet, in FIFO case, if HOL packet in Q_S belongs to flow B, no packet can be transmitted and wireless resources are wasted. □

Although HOL blocking in FIFO queues is a well-known problem, achievable throughput with FIFO queues in a wireless network is generally not known. In particular, stability region of a wireless network with FIFO queues as well as resource allocation schemes to achieve optimal operating points in the stability region are still open problems.

In this work, we investigate FIFO queues over wireless networks. We consider a wireless network model presented in Fig. 2 with multiple FIFO queues that are in the same transmission and interference range. (Note that this scenario is getting increasing interest in practice in the context of device-to-device and cooperative networks [7].) Our first step towards understanding the performance of FIFO queues in such a setup is to characterize the stability region of the network. Then, based on the structure of the stability region, we develop efficient resource allocation algorithms; *Deterministic FIFO-Control* (dFC) and *Queue-Based FIFO-Control* (qFC). The following are the key contributions of this work:

- We characterize the stability region of a general scenario where an arbitrary number of FIFO queues are shared by an arbitrary number of flows.
- The stability region of the FIFO queueing system under investigation is non-convex. Thus, we develop a convex inner-bound on the stability region, which is provably tight for certain operating points.
- We develop a resource allocation scheme; dFC, and a queue-based stochastic flow control and scheduling algorithm; qFC. We show that qFC achieves optimal operating point in the convex inner bound.
- We evaluate our schemes via simulations for multiple FIFO queues and flows. The simulation results show that our algorithms significantly improve the throughput as compared to the well-known queue-based flow control and max-weight scheduling schemes.

The structure of the rest of the paper is as follows. Section II gives an overview of the system model. Section III characterizes the stability region with FIFO queues. Section IV presents our resource allocation algorithms; dFC and qFC. Section V presents simulation results. Section VI presents related work. Section VII concludes the paper.

II. System Model

Wireless Network Setup: We consider a wireless network model presented in Fig. 2 with N FIFO queues. Let $\mathcal{N}$ be the set of FIFO queues, $\mathcal{Q}_n$ be the nth FIFO queue, and $\mathcal{K}_n$ be the set of flows passing through $\mathcal{Q}_n$. Also, let Q_n and K_n denote the cardinalities of sets $\mathcal{Q}_n$ and $\mathcal{K}_n$, respectively. We assume in our analysis that time is slotted, and t refers to the beginning of slot t.

Flow Rates: Each flow passing through $\mathcal{Q}_n$ and destined for node k is generated according to an arrival process $\lambda_{n,k}(t)$ at time slot t. The arrivals are i.i.d. over the time slots such that

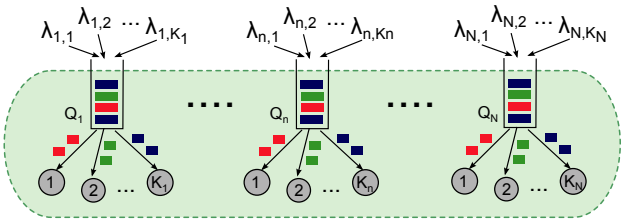

Fig. 2. The wireless network model that we consider in this paper. N FIFO queues share a wireless medium, where the nth FIFO queue, $\mathcal{Q}_n$ carries $\mathcal{K}_n$ flows towards their respective receiver nodes. The arrival rate of the kth flow passing through the nth queue is $\lambda_{n,k}$.

for every $n \in \mathcal{N}$ and $k \in \mathcal{K}_n$, we have $\lambda_{n,k} = E[\lambda_{n,k}(t)]$ and $E[\lambda_{n,k}(t)^2] < \infty$, where $E[\cdot]$ denotes the expected value.

Channel Model: In our setup in Fig. 2, as we mentioned earlier, we assume that all FIFO queues are in the same transmission and interference range, *i.e.,* only one FIFO queue could be served by a shared wireless medium at time t. On the other hand, a channel state from a FIFO queue to a receiver node may vary. In particular, at slot t, $\boldsymbol{C}(t) = \{C_{n,k}(t)\}_{\forall n \in \mathcal{N}, k \in \mathcal{K}_n}$ is the channel state vector, where $C_{n,k}(t)$ is the state of the link at time t from the nth queue $\mathcal{Q}_n$ to receiver node k such that $k \in \mathcal{K}_n$. The link state $C_{n,k}(t)$ takes values from the set $\{ON, OFF\}$ according to a probability distribution which is i.i.d. over time slots. If $C_{n,k}(t) = ON$, packets can be transmitted to receiver node k with rate $R_{n,k}$. We assume, for the sake of simplicity in this paper, that $R_{n,k} = 1$, and 1 packet can be transmitted at time slot t if $C_{n,k}(t) = ON$. If $C_{n,k}(t) = OFF$, no packets are transmitted. The ON and OFF probabilities of $C_{n,k}(t)$ are $\bar{p}_{n,k}$ and $p_{n,k}$, respectively. Note that $C_{n,k}(t)$ only determines the channel state; *i.e.,* the actual transmission opportunity from $\mathcal{Q}_n$ depends on the HOL packet as explained next.

Queue Structure and Evolution: Suppose that the Head-of-Line (HOL) packet of $\mathcal{Q}_n$ at time t is $H_n(t) \in \mathcal{K}_n$. The HOL packet together with the channel state defines the state of $\mathcal{Q}_n$. In particular, let $S_n(t)$ be the state of $\mathcal{Q}_n$ at time t such that $S_n(t) \in \{ON, OFF\}$. The state of $\mathcal{Q}_n$ is ON, *i.e.,* $S_n(t) = ON$ if $C_{n,H_n(t)} = ON$ at time t. Otherwise, $S_n(t) = OFF$. We define $\mathcal{S} = \{(S_1, \ldots, S_N) \mid S_1, \ldots, S_N \in \{ON, OFF\}\}$ as the set of the states of all FIFO queues.

Let us now consider the evolution of the HOL packet. If the state of queue $\mathcal{Q}_n$ is ON at time t, *i.e.,* $S_n(t) = ON$, the HOL packet can be transmitted (depending on the scheduling policy). If we assume that HOL packet is transmitted according to the scheduling policy, then a new packet is placed in the HOL position in $\mathcal{Q}_n$. The probability that this new HOL packet belongs to the kth flow is $\alpha_{n,k}$ and it depends on the arrival rates via $\alpha_{n,k} = \frac{\lambda_{n,k}}{\sum_{k \in \mathcal{K}_n} \lambda_{n,k}}$.

Now, we can consider the evolution of $\mathcal{Q}_n$. At time t, $\sum_{k \in \mathcal{K}_n} \lambda_{n,k}(t)$ packets arrive to $\mathcal{Q}_n$, and $g_n(t)$ packets are served according to the FIFO manner. Thus, queue size $Q_n(t)$ evolves according to the following dynamics.

$$Q_n(t+1) \leq \max[Q_n(t) - g_n(t), 0] + \sum_{k \in \mathcal{K}_n} \lambda_{n,k}(t). \quad (1)$$

Note that $g_n(t)$ depends on the states of the queues; $\mathcal{S}(t)$ at

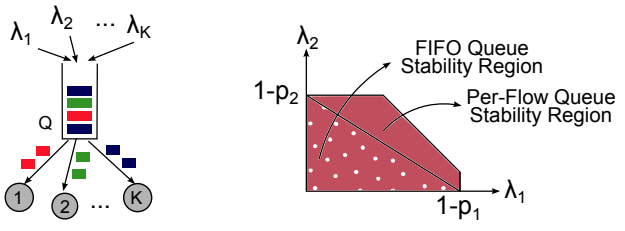

(a) FIFO queue (b) Stability region

Fig. 3. (a) Single-FIFO queue; $\mathcal{Q}$ is shared by K flows. (b) Stability region of a single-FIFO queue as well as per-flow queues with two flows.

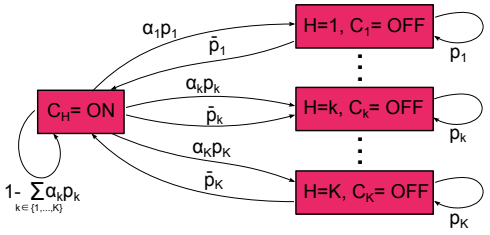

Fig. 4. Markov chain for the single-FIFO queue system shown in Fig 3(a).

time t, which characterize the stability region of the wireless network. Note that $\mathcal{S}(t)$ depends on arrival rates of flows to each FIFO queue; *i.e.*, $\lambda_{n,k}$ as well as the ON-OFF probability of each link, *i.e.*, $p_{n,k}$. In the next section, by taking into account $\lambda_{n,k}$ and $p_{n,k}$, we characterize the stability region of the wireless network.

III. Stability Region

In this section, our goal is to characterize the stability region of a wireless network where an arbitrary number of FIFO queues are served by a wireless medium. We first begin with the single-queue case shown in Fig. 3 to convey our approach for a canonical scenario, then we extend our stability region analysis for arbitrary number of FIFO queues and flows.

A. Single-FIFO Queue

We study the special case of a single FIFO queue $\mathcal{Q}_1$ where $\mathcal{N} = \{1\}$ with $N = 1$. For this special case, we thus drop the queue index n from the notation in Section II for brevity. In other words, we write $\mathcal{Q}$ instead of $\mathcal{Q}_n$, $C_k(t)$ instead of $C_{n,k}(t)$, and so on. Our main result in this context is then the following theorem.

Theorem 1: For a FIFO queue $\mathcal{Q}$ shared by $\mathcal{K} = \{1, \dots, K\}$ flows, if the channel states $C_k(t)$ and arrival rates $\lambda_k(t)$ are i.i.d. over time slots, the stability region Λ includes all arrival rates satisfying

$$\sum_{k\in\mathcal{K}} \frac{\lambda_k}{\bar{p}_k} \leq 1. \tag{2}$$

In other words, the stability region of the single-FIFO queue system is $\Lambda = \{\{\lambda_k\}_{k\in\mathcal{K}} |\ (2), \lambda_k \geq 0, \forall k \in \mathcal{K}\}$.

Proof: The state of the FIFO queue $\mathcal{Q}$ takes values from $\{ON, OFF\}$ depending the HOL packet and the states of the wireless links. Now, let us take a closer look at the FIFO states. The OFF state occurs if for some $k \in \mathcal{K} = \{1, \dots, K\}$ we have $H = k$ and $C_k = OFF$. Let z_k be the state that $H = k$ and $C_k = OFF$. We denote the probability of z_k as $P[z_k] = P[H = k, C_k = OFF]$. Also, let z_0 be the state that FIFO queue is at ON state for some HOL packet. The state z_0 happens precisely when the channel corresponding to the HOL packet is in the ON state. Therefore, the probability of z_0 is $P[z_0] = P[C_H = ON]$.

Having defined the queue state probabilities, we can observe that the packets from the FIFO queue could be served only at state z_0. It is also clear that the sum of the arrival rates to the queue $\mathcal{Q}$ should be less than the service rate, which is $P[z_0]$. Noting that we assumed $R_k = 1$, we conclude that $\sum_{k\in\mathcal{K}} \lambda_k \leq P[z_0]$.

Let us now calculate $P[z_0]$ and $P[z_k]$, $k \in \mathcal{K}$ using a Markov chain with states; z_0 and z_k, $k \in \mathcal{K}$. We first show that the state transition probability from z_0 to z_k is $P_{0,k} \triangleq \alpha_k p_k$, where $\alpha_k = \frac{\lambda_k}{\sum_{k\in\mathcal{K}} \lambda_k}$. Since we consider only one FIFO queue, when the queue is at state z_0, the HOL packet is always transmitted. The new HOL packet in the next state will belong to the kth flow with probability α_k, and $C_k = OFF$ with probability p_k. Therefore, the state transition probability from z_0 to z_k is $P_{0,k} = \alpha_k p_k$, as claimed.

The probability of moving from state z_k to z_0 is $P_{k,0} \triangleq \bar{p}_k$ as we can move to the unblocking state z_0 from the blocking state z_k if the channel is ON (with probability $\bar{p}_k$.). On the other hand, staying in the blocking state z_k is the OFF probability of the channel C_k. Thus, $P_{k,k} \triangleq p_k$. Note that the expressions for $P_{k,0}$ and $P_{k,k}$ do not involve the quantity α_k. The reason is that z_k is the blocking state, so when we move from z_k to another state (or staying at state z_k), the HOL packet is not transmitted and does not change (because $C_k = OFF$ at state z_k).

For any given $k, l \in \mathcal{K}$ with $k \neq l$, the state transition probability from z_k to z_l is $P_{k,l} \triangleq 0$. This follows since it is not possible to move from a blocking state to another (the HOL packet cannot be transmitted.). Finally, the probability of staying at state z_0 is $P_{0,0} \triangleq 1 - \sum_{k\in\mathcal{K}} \alpha_k p_k$ as the condition $\sum_{k=0}^{K} P_{0,k} = 1$ should be satisfied. The state transition probabilities are as shown in Fig. 4.

Now that we know the state transition probabilities of our Markov chain, we can calculate the balance equations, and these yield $P[z_0] = \frac{\sum_{k\in\mathcal{K}} \lambda_k}{\sum_{k\in\mathcal{K}} \lambda_k/\bar{p}_k}$. The calculations are provided in the following.

Let $P[\boldsymbol{z}] = \begin{bmatrix} P[z_0] & P[z_1] & \dots & P[z_K] \end{bmatrix}^T$. In the steady the state, the following set of equations are satisfied for the Markov Chain shown in Fig. 4.

$$P[\boldsymbol{z}]^T \begin{bmatrix} 1 - \sum_{k\in\mathcal{K}} \alpha_k p_k & \alpha_1 p_1 & \dots & \alpha_K p_K \\ \bar{p}_1 & p_1 & \dots & 0 \\ \bar{p}_2 & 0 & \dots & 0 \\ \vdots & \vdots & \ddots & \vdots \\ \bar{p}_k & 0 & \dots & p_K \end{bmatrix} = P[\boldsymbol{z}] \tag{3}$$

If we combine the $(k+1)$th equation in (3), which is $P[z_k] = P[z_0]\frac{\alpha_k p_k}{\bar{p}_k}$, and the fact that $P[z_0] + \sum_{k\in\mathcal{K}} P[z_k] = 1$, we have

$$P[z_0] = \frac{\sum_{k\in\mathcal{K}} \lambda_k}{\sum_{k\in\mathcal{K}} \lambda_k/\bar{p}_k} \tag{4}$$

We can then obtain $\sum_{k\in\mathcal{K}} \lambda_k \leq P[z_0] = \frac{\sum_{k\in\mathcal{K}} \lambda_k}{\sum_{k\in\mathcal{K}} \lambda_k/\bar{p}_k}$ which is equivalent to (2). This concludes the proof. ■

Example 2: Now suppose that single-FIFO queue $\mathcal{Q}$ is shared by two flows with rates λ_1 and λ_2. According to Theorem 1, the arrival rates should satisfy $\lambda_1/\bar{p}_1 + \lambda_2/\bar{p}_2 \leq 1$ for stability. This stability region is shown in Fig. 3(b). In the same figure, we also show the stability region of per-flow queues, [9]. As seen, the FIFO stability region is smaller as compared to per-flow capacity region. Yet, we still need flow control and scheduling algorithms to achieve the optimal operating point in this stability region. This issue will be discussed later in Section IV. □

B. Arbitrary Number of Queues and Flows

We now consider a wireless network with arbitrary number of FIFO queues and flows as shown in Fig. 2. The main challenge in this setup is that packet scheduling decisions affect the stability region. For example, if both $\mathcal{Q}_1$ and $\mathcal{Q}_n$ in Fig. 2 are at ON state, a decision about which queue to be served should be made. This decision affects future transmission opportunities from the queues, hence the stability region.

In this paper, we consider a scheduling policy where the packet transmission probability of each queue depends only on the queue states. In other words, if the state of the FIFO queues is $(S_1, \ldots, S_N) \in \mathcal{S}$, a packet from queue n is transmitted with probability $\tau_n(S_1, \ldots, S_N)$. We call this scheduling policy the *queue-state* policy. Note that as τ_n $(S_1, \ldots, S_N)$ is the transmission probability from queue $\mathcal{Q}_n$, we have the obvious constraint

$$\sum_{n\in\mathcal{N}} \tau_n(S_1, \ldots, S_N) \leq 1, \forall (S_1, \ldots, S_N) \in \mathcal{S}. \tag{5}$$

Our main result is then the following theorem.

Theorem 2: For a wireless network with N FIFO queues, if a queue-state policy τ_n is employed, then the stability region consists of the flow rates that satisfy

$$\lambda_{n,k} \leq \sum_{(S_1,\ldots,S_N)\in\mathcal{S}} \left\{ \frac{\lambda_{n,k} 1_{[S_n]}}{\sum_{k\in\mathcal{K}_n} \lambda_{n,k}/\bar{p}_{n,k}} \prod_{m\in\mathcal{N}-\{n\}} \left(\frac{\sum_{k\in\mathcal{K}_m} \lambda_{m,k}\rho_{m,k}(S_m)}{\sum_{k\in\mathcal{K}_m} \lambda_{m,k}/\bar{p}_{m,k}} \right) \tau_n(S_1, \ldots, S_N) \right\},$$
$$\forall n \in \mathcal{N}, k \in \mathcal{K}_n, \tag{6}$$

where

$$1_{[S_n]} = \begin{cases} 1, & S_n = ON \\ 0, & S_n = OFF \end{cases},$$

$$\rho_{m,k}(S_m) = \begin{cases} 1, & S_m = ON \\ p_{m,k}/\bar{p}_{m,k}, & S_m = OFF \end{cases}.$$

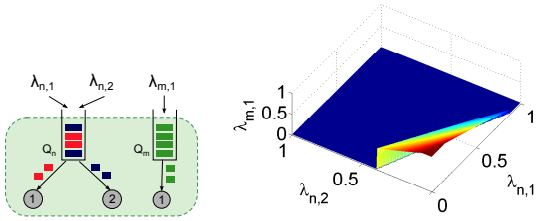

(a) Two FIFO Queues (b) Stability Region

Fig. 5. (a) Two FIFO queues; $\mathcal{Q}_n$ and $\mathcal{Q}_m$ are shared by two and one flows, respectively. (b) Three dimensional stability region with $\lambda_{n,1}$, $\lambda_{n,2}$ and $\lambda_{m,1}$ for the two-FIFO queues scenario shown in (a) when $p_{n,1} = 0.6$, $p_{n,2} = 0.1$, and $p_{m,1} = 0.7$.

Proof: The proof is provided in Appendix A. ■

The stability region of a FIFO queue system with N FIFO queues served by a wireless medium is characterized by $\Lambda = \{\{\lambda_{n,k}\}_{\forall n\in\mathcal{N}, k\in\mathcal{K}_n} |$ (6), (5), $\lambda_{n,k} \geq 0$, $n \in \mathcal{N}$, $k \in \mathcal{K}_n$, $\tau_n(S_1, \ldots, S_N) \geq 0$, $\forall\, n \in \mathcal{N}, (S_1, \ldots, S_N) \in \mathcal{S}\}$.

Example 3: Now let us consider two FIFO queues $\mathcal{Q}_n$ and $\mathcal{Q}_m$ which are shared by three flows with rates; $\lambda_{n,1}$, $\lambda_{n,2}$, and $\lambda_{m,1}$ (Fig. 5(a)). According to Theorem 2, the stability region Λ should include arrival rates satisfying inequalities in (6) and (5). In this example, with two queues and three flows, these inequalities are equivalent to

$$\lambda_{n,1} + \lambda_{n,2} + \lambda_{m,1} \leq \left(\frac{p_{m,1}(\lambda_{n,1} + \lambda_{n,2})}{\lambda_{n,1}/\bar{p}_{n,1} + \lambda_{n,2}/\bar{p}_{n,2}}\right) + \bar{p}_{m,1} \tag{7}$$

with $\lambda_{n,1}/\bar{p}_{n,1} + \lambda_{n,2}/\bar{p}_{n,2} \leq 1$, and $\lambda_{m,1}/\bar{p}_{m,1} \leq 1$. The stability region corresponding to these inequalities is the region below the surface in Fig. 5(b). [1] □

In general, we wish to find the optimal operating points on the boundary of the stability region Λ. However, the stability region may not be convex for arbitrary number of queues and flows. Developing a convex inner bound on the stability region is crucial for developing efficient resource allocation algorithms for wireless networks with FIFO queues. We thus next propose a convex inner bound on the stability region.

C. A Convex Inner Bound on the Stability Region:

Let us consider a flow with arrival rate $\lambda_{n,k}$ to the FIFO queue $\mathcal{Q}_n$. If there are no other flows and queues in the network, then the arrival rate should satisfy $\lambda_{n,k}/\bar{p}_{n,k} \leq 1$ according to Theorem 2. In this formulation, $\lambda_{n,k}/\bar{p}_{n,k}$ is the total amount of wireless resources that should be allocated to transmit the flow with rate $\lambda_{n,k}$. For multiple-flow, single-FIFO case, the stability region is $\sum_{k\in\mathcal{K}_n} \lambda_{n,k}/\bar{p}_{n,k} \leq 1$. Similar to the single-flow case, $\lambda_{n,k}/\bar{p}_{n,k}$ term is the amount of wireless resources that should be allocated to the kth flow. Finally, for the general stability region for arbitrary number of queues and flows, let us consider (6) again. Assuming $\psi_m(S_m) = \frac{\sum_{k\in\mathcal{K}_m} \lambda_{m,k}\rho_{m,k}(S_m)}{\sum_{k\in\mathcal{K}_m} \lambda_{m,k}/\bar{p}_{m,k}}$, we can write $\sum_{k\in\mathcal{K}_n} \lambda_{n,k}$

[1] Note that the time sharing argument to convexify the stability region does not apply to this scenario, because the non-convexity comes from the relationship among the arrival rates instead of the service rates from the FIFO queues. Thus, the centralized time-sharing for the arrival rates is not practical.

from (6) as;

$$\sum_{k\in\mathcal{K}_n}\lambda_{n,k} \le \sum_{(S_1,\ldots,S_N)\in\mathcal{S}} \Bigg\{ \frac{\sum_{k\in\mathcal{K}_n}\lambda_{n,k}1_{[S_n]}}{\sum_{k\in\mathcal{K}_n}\lambda_{n,k}/\bar{p}_{n,k}} \prod_{m\in\mathcal{N}-\{n\}}\psi_m(S_m)\tau_n(S_1,\ldots,S_N)\Bigg\}, \forall n\in\mathcal{N}, k\in\mathcal{K}_n \quad (8)$$

which, assuming that $\sum_{k\in\mathcal{K}_n}\lambda_{n,k}>0$, is equivalent to

$$\sum_{k\in\mathcal{K}_n}\lambda_{n,k}/\bar{p}_{n,k} \le \sum_{(S_1,\ldots,S_N)\in\mathcal{S}} 1_{[S_n]} \prod_{m\in\mathcal{N}-\{n\}}\psi_m(S_m) \tau_n(S_1,\ldots,S_N), \forall n\in\mathcal{N}, k\in\mathcal{K}_n \quad (9)$$

Intuitively speaking, the right hand side of (9) corresponds to the amount of wireless resources that is allocated to the nth queue $\mathcal{Q}_n$. Thus, similar to the single-FIFO queue, we can consider that $\lambda_{n,k}/\bar{p}_{n,k}$ term corresponds to the amount of wireless resources that should be allocated to the kth flow.

Our key point while developing an inner bound on the stability region is to provide rate fairness across competing flows in each FIFO queue. Since each flow requires $\lambda_{n,k}/\bar{p}_{n,k}$ amount of wireless resources; it is intuitive to have the following equality $\lambda_{n,k}/\bar{p}_{n,k} = \lambda_{n,l}/\bar{p}_{n,l}$, $k\neq l$ to fairly allocate wireless resources across flows. More generally, we define a function $a_n = \lambda_{n,k}/(\bar{p}_{n,k})^\beta$, $\forall k\in\mathcal{K}_n$ where $\beta\ge 1$, and we develop a stability region for a_n instead of $\lambda_{n,k}$. The role of the exponent β is to provide flexibility to the targeted fairness. For example, if we want to allocate more resources to flows with better channels, then β should be larger.

Now, by the definition of a_n, we have the equivalent form

$$a_n \le \sum_{(S_1,\ldots,S_N)\in\mathcal{S}} \frac{1_{[S_n]}}{\sum_{k\in\mathcal{K}_n}(\bar{p}_{n,k})^{\beta-1}} \prod_{m\in\mathcal{N}-\{n\}}\omega_m(S_m) \tau_n(S_1,\ldots,S_N), \forall n\in\mathcal{N} \quad (10)$$

of (6), where $\omega_m(S_m) = \frac{\sum_{k\in\mathcal{K}_m}(\bar{p}_{m,k})^\beta \rho_{m,k}(S_m)}{\sum_{k\in\mathcal{K}_m}(\bar{p}_{m,k})^{\beta-1}}$. As seen, (10) is a convex function of a_n. Thus, we can define the region $\tilde{\Lambda} = \{\{a_n\}_{n\in\mathcal{N}} |$ (10), (5), $a_n\ge 0, \tau_n(S_1,\ldots,S_N)\ge 0, \forall n\in\mathcal{N}, (S_1,\ldots,S_N)\in\mathcal{S}\}$, which is clearly an inner bound on the actual stability region Λ. Despite the fact that $\tilde{\Lambda}$ is only inner bound on Λ, for some operating points, *i.e.,* at the intersection of $\lambda_{n,k}/\bar{p}_{n,k} = \lambda_{n,l}/\bar{p}_{n,l}$, $k\neq l$ lines, the two stability regions ($\tilde{\Lambda}$ and Λ) coincide. Thus, for some utility functions, optimal operating points in both $\tilde{\Lambda}$ and Λ coincide. In the next section, we develop resource allocation schemes; dFC and qFC that achieve utility optimal operating points in $\tilde{\Lambda}$.

IV. Flow Control and Scheduling

In this section, we develop resource allocation schemes; *deterministic FIFO-Control* (dFC), and a *queue-based FIFO control* (qFC).

In general, our goal is to solve the optimization problem

$$\max_{\boldsymbol{\lambda}} \sum_{n\in\mathcal{N}}\sum_{k\in\mathcal{K}_n} U_{n,k}(\lambda_{n,k}) \quad \text{s.t. } \lambda_{n,k}\in\Lambda, n\in\mathcal{N}, k\in\mathcal{K}_n \quad (11)$$

and to find the corresponding optimal rates, where $U_{n,k}$ is a concave utility function assigned to flow with rate $\lambda_{n,k}$. Although the objective function $\sum_{n\in\mathcal{N}}\sum_{k\in\mathcal{K}_n}U_{n,k}(\lambda_{n,k})$ in (11) is concave, the optimization domain Λ (*i.e.,* the stability region) may not be convex. Thus, we convert this problem to a convex optimization problem based on the structure of the inner bound we have developed in Section III-C. In particular, setting $a_n = \lambda_{n,k}/(\bar{p}_{n,k})^\beta$, the problem in (11) reduces to $\max_{\boldsymbol{a}}\sum_{n\in\mathcal{N}}\sum_{k\in\mathcal{K}_n}U_n(a_n(\bar{p}_{n,k})^\beta)$, $a_n\in\tilde{\Lambda}, n\in\mathcal{N}$. This is our deterministic FIFO-control scheme; dFC and expressed explicitly as;

Deterministic FIFO-Control (dFC):

$$\begin{aligned}\max_{\boldsymbol{a},\tau}\ & \sum_{n\in\mathcal{N}}\sum_{k\in\mathcal{K}_n}U_{n,k}(a_n(\bar{p}_{n,k})^\beta)\\ \text{s.t. } a_n \le & \sum_{(S_1,\ldots,S_N)\in\mathcal{S}}\frac{1_{[S_n]}}{\sum_{k\in\mathcal{K}_n}(\bar{p}_{n,k})^{\beta-1}} \prod_{m\in\mathcal{N}-\{n\}}\omega_m(S_m)\tau_n(S_1,\ldots,S_N), \forall n\in\mathcal{N}\\ & \sum_{n\in\mathcal{N}}\tau_n(S_1,\ldots,S_N)\le 1, \forall (S_1,\ldots,S_N)\in\mathcal{S}\\ & a_n\ge 0, \forall n\in\mathcal{N}, (S_1,\ldots,S_N)\in\mathcal{S}\\ & \tau_n(S_1,\ldots,S_N)\ge 0, \forall n\in\mathcal{N}, (S_1,\ldots,S_N)\in\mathcal{S} \quad (12)\end{aligned}$$

Note that dFC optimizes a_n and $\tau_n(S_1,\ldots,S_N)$. After the optimal values are determined, packets are inserted into the FIFO queue $\mathcal{Q}_n$ depending on $\lambda_{n,k} = a_n(\bar{p}_{n,k})^\beta$ and served from the FIFO queue $\mathcal{Q}_n$ depending on $\tau_n(S_1,\ldots,S_N)$.

Although dFC gives us optimal operating points in the stability region; $\tilde{\Lambda}$, it is a centralized solution, and its adaptation to varying wireless channel conditions is limited. Thus, we also develop a more practical and queue-based FIFO-control scheme qFC, next.

Queue-Based FIFO-Control (qFC):

- *Flow Control:* At every slot t, the flow controller attached to the FIFO queue $\mathcal{Q}_n$ determines $a_n(t)$ according to;

$$\max_{\boldsymbol{a}}\ M\big[\sum_{k\in\mathcal{K}_n}U_{n,k}(a_n(t)(\bar{p}_{n,k})^\beta)\big] - Q_n(t)a_n(t) \quad \text{s.t. } a_n(t)\le R_n^{max}, a_n(t)\ge 0 \quad (13)$$

  where M is a large positive number, and R_n^{max} is a positive value larger than the maximum outgoing rate from FIFO queue $\mathcal{Q}_n$ (which is $R_n^{max}>1$ as we assume that the maximum outgoing rate from a queue is 1 packet per slot). After $a_n(t)$ is determined according to (13), $\lambda_{n,k}(t)$ is set as $\lambda_{n,k}(t) = a_n(t)\ (\bar{p}_{n,k})^\beta$. Then, $\lambda_{n,k}(t)$ packets from the kth flow are inserted in $\mathcal{Q}_n$.
- *Scheduling:* At slot t, the scheduling algorithm determines the FIFO queue from which a packet is transmitted according to;

$$\max_{\boldsymbol{\tau}}\ \sum_{n\in\mathcal{N}}Q_n(t)\frac{1_{[S_n(t)]}}{\sum_{k\in\mathcal{K}_n}(\bar{p}_{n,k})^\beta}\tau_n(S_1(t),\ldots,S_N(t)) \quad \text{s.t. } \sum_{n\in\mathcal{N}}\tau_n(S_1(t),\ldots,S_N(t))\le 1,$$

$$\tau_n(S_1(t),\ldots,S_N(t)) \geq 0 \tag{14}$$

After $\tau_n(S_1(t),\ldots,S_N(t))$ is determined, the outgoing traffic rate from queue $\mathcal{Q}_n$ is set to $g_n(t) = \tau_n\ (S_1(t),\ \ldots,\ S_N(t))\ 1_{[S_n(t)]}$, and $g_n(t)$ packets (which is 1 or 0 in our case) are transmitted from $\mathcal{Q}_n$.

Thus, the queue dynamics change according to (1) and based on (13) and (14). Such queue dynamics lead to the following result.

Theorem 3: If the channel states are i.i.d. over time slots, the traffic arrival rates are controlled by the rate control algorithm in (13), and the FIFO queues are served by the scheduling algorithm in (14), then the admitted flow rates converge to the utility optimal operating point in the stability region $\tilde{\Lambda}$ with increasing M.

Proof: The proof is provided in Appendix B. □

V. Performance Evaluation

In this section, we evaluate our dFC and qFC algorithms as compared to the baselines; (i) *optimal* solution, and (ii) *max-weight* algorithm for different number of FIFO queues and flows. Next, we briefly explain our baselines.

A. Baselines

The *optimal* solution is a solution to (11), and we compared dFC and qFC with the *optimal* solution for some scenarios where the stability region Λ is convex. On the other hand, *max-weight* algorithm is a queue-based flow control and max-weight scheduling scheme. Our baseline *max-weight* algorithm mimics the structure of the solution provided in [5], and it is summarized briefly in the following.

Max-weight for FIFO:

- *Flow Control:* At every time slot t, the flow controller attached to the FIFO queue $\mathcal{Q}_n$ determines $\lambda_{n,k}(t)$ according to;

$$\max_{\boldsymbol{\lambda}}\ M\big[\sum_{k\in\mathcal{K}_n} U_{n,k}(\lambda_{n,k}(t))\big] - Q_{n,k}(t)\lambda_{n,k}(t)$$
$$\text{s.t. } \lambda_{n,k}(t) \leq R^{max}_{n,k}, \forall k \in \mathcal{K}_n \tag{15}$$

  where M and $R^{max}_{n,k}$ are positive large constants similar to (13), and $Q_{n,k}(t)$ is the number of packets that belong to the kth flow in queue $\mathcal{Q}_n$.
- *Scheduling:* At slot t, the scheduling algorithm determines the FIFO queue from which a packet is transmitted according to;

$$\max_{\boldsymbol{\tau}}\ \sum_{n\in\mathcal{N}} Q_n(t)1_{[S_n(t)]}\tau_n(S_1(t),\ldots,S_N(t))$$
$$\text{s.t. } \sum_{n\in\mathcal{N}} \tau_n(S_1(t),\ldots,S_N(t)) \leq 1$$
$$\tau_n(S_1(t),\ldots,S_N(t)) \geq 0 \tag{16}$$

  After $\tau_n\ (S_1(t),\ \ldots,\ S_N(t))$ is determined, a packet from the queue $\mathcal{Q}_n$ is transmitted if $\tau_n\ (S_1(t),\ \ldots,\ S_N(t)) = 1$; no packet is transmitted, otherwise.

Next, we present our simulation results for single and multiple FIFO queues.

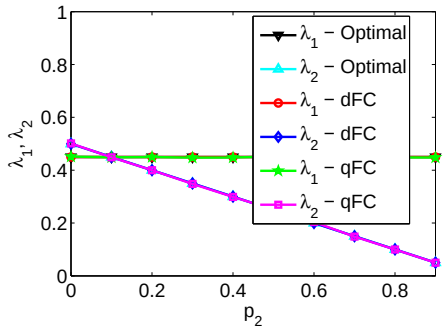

(a) Per-flow rates

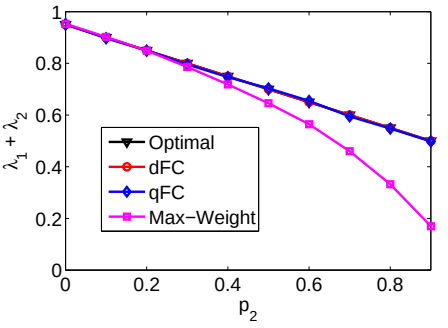

(b) Total rate

Fig. 6. Single-FIFO queue shared by two flows when $p_1 = 0.1$, $\beta = 1$, and $U_k(\lambda_k) = \log(\lambda_k)$. (a) Per-flow rates vs. p_2. (b) Total flow rate vs. p_2.

B. Single-FIFO Queue

In this section, we consider a single FIFO queue $\mathcal{Q}_1$. Similar to Section III-A, we drop the queue index $n = 1$ from the notation for brevity. In other words, we write λ_k instead of $\lambda_{1,k}$, p_k instead of $p_{1,k}$, and so on.

Fig. 6 presents simulation results for a single queue and two flows for $p_1 = 0.1$, $\beta = 1$, and $U_k(\lambda_k) = \log(\lambda_k)$. Fig. 6(a) shows per-flow rates; λ_1 and λ_2 when p_2 is increasing. As seen, λ_1 is the same for all algorithms; optimal, dFC, and qFC. This also holds for λ_2. These results show that our algorithms dFC and qFC are as good as the optimal solution, and achieve the optimal operating points in Λ in this scenario. The simulations results also show that our algorithms reduce the second flow rate λ_2 when p_2 increases while λ_1 and p_1 do not change. This means that our algorithms do not penalize a flow (flow 1) when the channel of another competing flow (flow 2) deteriorates, which shows the effectiveness of our algorithms to provide fairness.

Fig. 6(b) shows the total rate $\lambda_1 + \lambda_2$ versus p_2 for the same setup. As seen, our algorithms improves throughput over max-weight significantly. This is expected as our algorithms are designed to reduce the HOL blocking and to allocate wireless resources fairly among multiple flows.

Fig. 7 shows simulation results for a single queue shared by multiple flows. In this setup, p_k is selected randomly between $[0, 1]$, $\beta = 1$, $U_k(\lambda_k) = \log(\lambda_k)$. The simulations are repeated for 1000 different seeds, and the average values are reported. Fig. 7(a) shows average flow rate versus number of flows for our algorithms as well as max-weight. As seen,

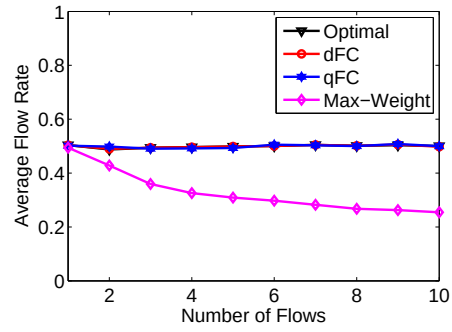

(a) Flow rates

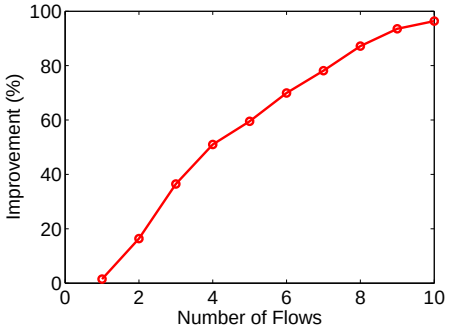

(b) Throughput improvement

Fig. 7. Single-FIFO queue shared by multiple flows. p_k is selected randomly between $[0, 1]$, $\beta = 1$, and $U_k(\lambda_k) = \log(\lambda_k)$. (a) Average flow rate versus number of flows. (b) Percentage of throughput improvement of qFC over max-weight.

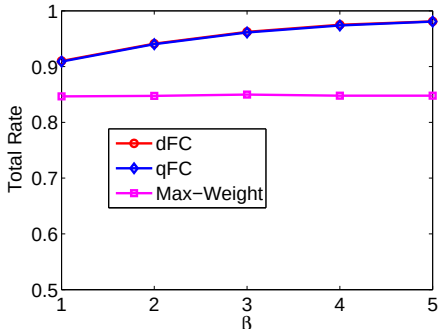

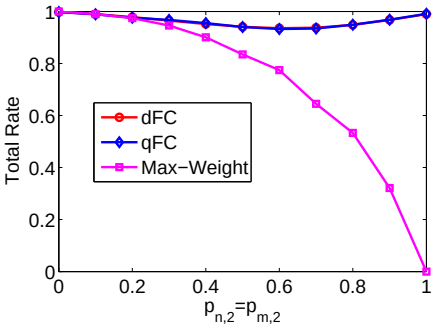

Fig. 8. Two FIFO queues with four flows. (a) Total flow rate versus β when $p_{n,1} = 0.1$, $p_{n,1} = 0.5$, $p_{m,1} = 0.1$, $p_{m,2} = 0.5$, and log utility is employed, *i.e.*, $U_{n,k}(\lambda_{n,k}) = \log(\lambda_{n,k})$. (b) Total rate versus $p_{n,2} = p_{m,2}$ when $p_{n,1} = p_{m,1} = 0.1$ and $\beta = 2$.

dFC and qFC are as good as the optimal solution, and they improve over max-weight significantly. Fig. 7(b) shows the same simulation results, but reports the improvement of qFC over max-weight. This figure shows that the improvement of our algorithms increases with increasing number of flows. Indeed, the improvement is up to 100% when $K = 10$, which is significant. The improvement is higher for large number of flows, because our algorithm allocates resources to the flows based on the quality of their channels and reduces the flow rate for the flows with bad channel conditions. However, max-weight does not have such a mechanism, and when there are more flows in the system, the probability of having a flow with bad channel condition increases, which reduces the overall throughput.

C. Two-FIFO Queues

In this section, we consider two FIFO queues $\mathcal{Q}_m$ and $\mathcal{Q}_n$. There are four flows in the system and each queue carries two flows, *i.e.*, $\mathcal{Q}_n$ carries flows with rates $\lambda_{n,1}$, $\lambda_{n,2}$ and $\mathcal{Q}_m$ carries flows with rates $\lambda_{m,1}$, $\lambda_{m,2}$.

Fig. (8)(a) shows the total flow rate versus β for the scenario of two-FIFO queues with four flows when $p_{n,1} = 0.1$, $p_{n,2} = 0.5$, $p_{m,1} = 0.1$, $p_{m,2} = 0.5$, and log utility is employed, *i.e.*, $U_{n,k}(\lambda_{n,k}) = \log(\lambda_{n,k})$. (We do not present the results of the optimal solution as the stability region Λ is not convex in this scenario.) As seen, dFC and qFC have the same performance and improve over max-weight. The improvement increases with increasing β as dFC and qFC penalize flows with bad channel conditions more when β increases, which increases the total throughput.

Fig. (8)(b) shows the total rate versus $p_{n,2} = p_{m,2}$ for two-FIFO queues with four flows when $p_{n,1} = p_{m,1} = 0.1$ and $\beta = 2$. As seen, dFC and qFC improve significantly over max-weight. Furthermore, they achieve almost maximum achievable rate 1 all the time. The reason is that dFC and qFC penalizes the queues with with bad channels. For example, when $p_{n,2} = p_{m,2} = 1$, the total rate is 1, because they allocate all the resources to $\lambda_{n,1}$ and $\lambda_{m,1}$ as there is no point to allocate those resources to $\lambda_{n,2}$ and $\lambda_{m,2}$ since their channels are always OFF. On the other hand, max-weight does not arrange the flow and queue service rates based on the channel conditions, so the total rate reduces to 0 when $p_{n,2} = p_{m,2} = 1$, *i.e.*, it is not possible to transmit any packets when max-weight is employed in this scenario.

Fig. 9 further demonstrates how our algorithms treat flows with bad channel conditions. In particular, Fig. 9 presents per-flow rate versus $p_{m,2}$ for the scenario of two-FIFO queues with four flows when $p_{n,1} = p_{n,2} = p_{m,1} = 0$ and $\beta = 2$ for (a) dFC and qFC and (b) max-weight. As seen, when $p_{m,2}$ increases, $\lambda_{m,2}$ decreases in Fig. 9(a) since its channel is getting worse. Yet, this does not affect the other flows. In fact, $\lambda_{m,1}$ even increases as more resources are allocated to it when $p_{m,2}$ increases. On the other hand, both $\lambda_{m,1}$ and $\lambda_{m,2}$ decrease with increasing $p_{m,2}$ in max-weight (Fig. 9(b)). This is not fair, because $\lambda_{m,1}$ decreases with increasing $p_{m,2}$ although its channel is always ON as $p_{m,1} = 0$. In the same scenario (Fig. 9(b)), the rates of the nth queue ($\lambda_{n,1}$ and $\lambda_{n,2}$)

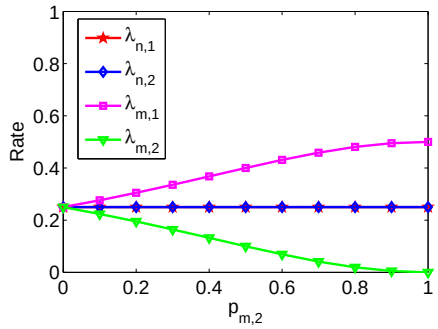

(a) dFC and qFC

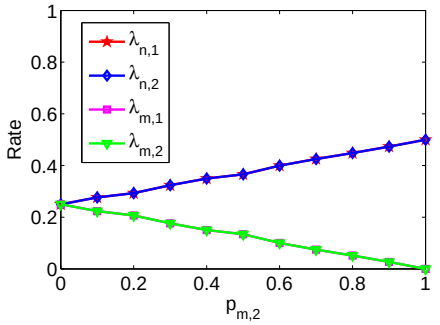

(b) Max-weight

Fig. 9. Per-flow rates versus $p_{m,2}$ for the scenario of two-FIFO queues with four flows when $p_{n,1} = p_{n,2} = p_{m,1} = 0$ and $\beta = 2$. (a) dFC and qFC. (b) Max-weight.

increase with increasing $p_{m,2}$ as they use available resource opportunistically. This makes the total rate the same for dFC, qFC, and max-weight. Yet, as we discussed, max-weight is not fair to flow $\lambda_{m,1}$ in this scenario.

VI. Related Work

In this work, our goal is to understand FIFO queues in wireless networks and develop efficient flow control and scheduling policies for such a setup. In the seminal paper [8], the authors analyze FIFO queues in an input queued switch. They show that the use of FIFO queues in that context limits the throughput to approximately 58% of the maximum achievable throughput. However, in the context of wireless networks, similar results are in general not known.

Backpressure routing and scheduling framework has emerged from the pioneering work [3], [4], which has generated a lot of research interest [9]; especially for wireless ad-hoc networks [10]–[15]. Furthermore, it has been shown that backpressure can be combined with flow control to provide utility-optimal operation guarantee [5], [14]. Such previous work mainly considered per-flow queues. However, FIFO queueing structure, which is the focus of this paper, is not compatible with the per-flow queueing requirements of these routing and scheduling schemes.

The strengths of backpressure-based network control have recently received increasing interest in terms of practical implementation. Multi-path TCP scheme is implemented over wireless mesh networks in [16] for routing and scheduling packets using a backpressure based heuristic. At the link layer, [17]–[19] propose, analyze, and evaluate link layer backpressure-based implementations with queue prioritization and congestion window size adjustment. Backpressure is implemented over sensor networks [20] and wireless multi-hop networks [21]. In these schemes, either last-in, first-out queueing is employed [20] or link layer FIFO queues are strictly controlled [21] to reduce the number of packets in the FIFO queues, hence HOL blocking.

In backpressure, each node constructs per-flow queues. There is some work in the literature to stretch this necessity. For example, [22], [23] propose using real per-link and virtual per-flow queues. Such a method reduces the number of queues required in each node, and reduces the delay, but it still needs to construct per-link queues. Similarly, [24] constructs per-link queues in the link layer, and schedule packets according to FIFO rule from these queues. Such a setup is different than ours as per-link queues do not introduce HOL blocking.

The main differences in our work are: (i) we consider FIFO queues shared by multiple flows where HOL blocking occurs as each flow is transmitted over a possibly different wireless link, (ii) we characterize the stability region of a general scenario where an arbitrary number of FIFO queues, which are served by a wireless medium, are shared by an arbitrary number of flows, and (iii) we develop efficient resource allocation schemes to exploit achievable rate in such a setup.

VII. Conclusion

We investigated the performance of FIFO queues over wireless networks and characterized the stability region of this system for arbitrary number of FIFO queues and flows. We developed inner bound on the stability region, and developed resource allocation schemes; dFC and qFC, which achieve optimal operating point in the convex inner bound. Simulation results show that our algorithms significantly improve throughput in a wireless network with FIFO queues as compared to the well-known queue-based flow control and max-weight scheduling schemes.

References

[1] Cisco Visual Networking Index: Global Mobile Data Traffic Forecast Update, 2010 - 2015.

[2] Ericsson Mobility Report, November 2013.

[3] L. Tassiulas and A. Ephremides, "Stability properties of constrained queueing systems and scheduling policies for maximum throughput in multihop radio networks," *IEEE Trans. Autom. Control*, vol. 37, no. 12, pp. 1936–1948, Dec. 1992.

[4] L. Tassiulas and A. Ephremides, "Dynamic server allocation to parallel queues with randomly varying connectivity," *IEEE Trans. Inf. Theory*, vol. 39, no. 2, pp. 466–478, Mar. 1993.

[5] M. J. Neely, E. Modiano, and C. Li, "Fairness and optimal stochastic control for heterogeneous networks," *IEEE/ACM Trans. Net.*, vol. 16, no. 2, pp. 396–409, Apr. 2008.

[6] http://madwifi-project.org/wiki/Chipsets.

[7] L. Keller, A. Le, B. Cici, H. Seferoglu, C. Fragouli, A. Markopoulou, "MicroCast: Cooperative Video Streaming on Smartphones," *ACM MobiSys*, June 2012.

[8] M. J. Karol, M. G. Hluchyj, and S. P. Morgan, "Input versus output queueing on a space-division packet switch," *IEEE Trans. Commun.*, vol. 35, no. 12, pp. 1347–1356, Dec. 1987.

[9] M. J. Neely, *Stochastic Network Optimization with Application to Communication and Queueing Systems*, Morgan & Claypool, 2010.
[10] L. Tassiulas, "Scheduling and performance limits of networks with constantly changing topology," *IEEE Trans. Inf. Theory*, vol. 43, no. 3, pp. 1067–1073, May 1997.
[11] N. Kahale and P. E. Wright, "Dynamic global packet routing in wireless networks," *IEEE INFOCOM*, Apr. 1997.
[12] M. Andrews, K. Kumaran, K. Ramanan, A. Stolyar, P. Whiting, and R. Vijaykumar, "Providing quality of service over a shared wireless link," *IEEE Commun. Mag.*, vol. 39, no. 2, pp. 150–154, Feb. 2001.
[13] M. J. Neely, E. Modiano, and C. E. Rohrs, "Dynamic power allocation and routing for time varying wireless networks," *IEEE J. Select. Areas Commun.*, vol. 23, no. 1, pp. 89–103, Jan. 2005.
[14] A. L. Stolyar, "Greedy primal dual algorithm for dynamic resource allocation in complex networks," *Queuing Systems*, vol. 54, no. 3, pp. 203–220, 2006.
[15] J. Liu, A. L. Stolyar, M. Chiang, and H. V. Poor, "Queue backpressure random access in multihop wireless networks: optimality and stability," *IEEE Trans. Inf. Theory*, vol. 55, no. 9, pp. 4087–4098, Sept. 2009.
[16] B. Radunovic, C. Gkantsidis, D. Gunawardena, and P. Key, "Horizon: balancing TCP over multiple paths in wireless mesh network," *ACM MobiCom*, Sept. 2008.
[17] A. Warrier, S. Janakiraman, S. Ha, I. Rhee, "DiffQ: practical differential backlog congestion control for wireless networks," *IEEE INFOCOM*, Apr. 2009.
[18] U. Akyol, M. Andrews, P. Gupta, J. Hobby, I. Saniee, and A. Stolyar, "Joint scheduling and congestion control in mobile ad-hoc networks," *IEEE INFOCOM*, Apr. 2008.
[19] A. Sridharan, S. Moeller, B. Krishnamachari, "Making distributed rate control using Lyapunov drifts a reality in wireless sensor networks," *IEEE WiOpt*, Apr. 2008.
[20] S. Moeller, A. Sridharan, B. Krishnamachari, and O. Gnawali, "Routing without routes: the backpressure collection protocol," *ACM IPSN*, Apr. 2010.
[21] R. Laufer, T. Salonidis, H. Lundgren, and P. L. Guyadec, "XPRESS: a cross-layer backpressure architecture for wireless multi-hop networks," *ACM MobiCom*, Sept. 2011.
[22] E. Athanasopoulou, L. X. Bui, T. Ji, R. Srikant, and A. Stolyar, "Backpressure-based packet-by-packet adaptive routing in communication networks," *IEEE/ACM Trans. Net.*, vol. 21, no. 1, pp. 244–257, Feb. 2013.
[23] L. X. Bui, R. Srikant, and A. Stolyar, "A novel architecture for reduction of delay and queueing structure complexity in the back-pressure algorithm," *IEEE/ACM Trans. Net.*, vol. 19, no. 6, pp. 1597–1609, Dec. 2011.
[24] H. Seferoglu, E. Modiano, "Diff-Max: Separation of Routing and Scheduling in Backpressure-Based Wireless Networks," *IEEE INFOCOM*, Apr. 2013.

APPENDIX A: PROOF OF THEOREM 2

In this section, we provide a proof of Theorem 2 for arbitrary number of FIFO queues and flows. Let us first consider $\lambda_{n,k}$, which should satisfy the following inequality.

$$\lambda_{n,k} \leq \sum_{(S_1,\ldots,S_N)\in\mathcal{S}} P[S_1,\ldots,S_N,H_n=k]1_{[S_n]} \tau_n(S_1,\ldots,S_N), \forall n\in\mathcal{N}, k\in\mathcal{K}_n. \quad (17)$$

where $P[S_1,\ldots,S_N,H_n=k]$ is the probability that the states of the queues are $(S_1,\ldots,S_N)$ and $H_n=k$, which is required as we can transmit a packet from the kth flow only when the HOL packet belongs to the kth flow. In this equation, we can calculate $P[S_1,\ldots,S_N,H_n=k]$ as

$$P[S_1,\ldots,S_N,H_n=k] = \sum_{l_1\in\mathcal{K}_1}\cdots\sum_{l_{n-1}\in\mathcal{K}_{n-1}}\sum_{l_{n+1}\in\mathcal{K}_{n+1}}\cdots \sum_{l_N\in\mathcal{K}_N} P[S_1,\ldots,S_N,H_n=k,H_1=l_1,\ldots,H_{n-1}=l_{n-1}, H_{n+1}=l_{n+1},\ldots,H_N=l_N], \quad (18)$$

$$P[S_1,\ldots,S_N,H_n=k] = \sum_{l_1\in\mathcal{K}_1}\cdots\sum_{l_{n-1}\in\mathcal{K}_{n-1}}\sum_{l_{n+1}\in\mathcal{K}_{n+1}}\cdots \sum_{l_N\in\mathcal{K}_N} \underbrace{P[S_1|H_1=l_1]}_{\triangleq\xi_{1,l_1}(S_1)}\cdots\underbrace{P[S_{n-1}|H_{n-1}=l_{n-1}]}_{\triangleq\xi_{n-1,l_{n-1}}(S_{n-1})} \underbrace{P[S_n|H_n=k]}_{\triangleq\xi_{n,k}(S_n)}\underbrace{P[S_{n+1}|H_{n+1}=l_{n+1}]}_{\triangleq\xi_{n+1,l_{n+1}}(S_{n+1})}\cdots\underbrace{P[S_N|H_N=l_N]}_{\triangleq\xi_{N,l_N}(S_N)} P[H_n=k,H_1=l_1,\ldots,H_{n-1}=l_{n-1},H_{n+1}=l_{n+1},\ldots, H_N=l_N] \quad (19)$$

Thus, we have

$$P[S_1,\ldots,S_N,H_n=k] = \sum_{l_1\in\mathcal{K}_1}\cdots\sum_{l_{n-1}\in\mathcal{K}_{n-1}}\sum_{l_{n+1}\in\mathcal{K}_{n+1}}\cdots \sum_{l_N\in\mathcal{K}_N}\xi_{1,l_1}(S_1)\ldots\xi_{n-1,l_{n-1}}(S_{n-1})\xi_{n,k}(S_n) \xi_{n+1,l_{n+1}}(S_{n+1})\ldots\xi_{N,l_N}(S_N)P[H_n=k,H_1=l_1,\ldots, H_{n-1}=l_{n-1},H_{n+1}=l_{n+1},\ldots,H_N=l_N]. \quad (20)$$

Now, we should calculate $P[H_n=k,H_1=l_1,\ldots,H_{n-1}=l_{n-1},H_{n+1}=l_{n+1},\ldots,H_N=l_N]$.

We claim that $P[H_n=k,\ H_1=l_1,\ \ldots,\ H_{n-1}=l_{n-1},\ H_{n+1}=l_{n+1},\ \ldots,\ H_N=l_N] = P[H_1=l_1]\ \ldots\ P[H_{n-1}=l_{n-1}]\ P[H_n=k]\ P[H_{n+1}=l_{n+1}]\ \ldots\ P[H_N=l_N]$. To prove this claim, we should show, without loosing generality, that the following conditions hold.

$$\begin{aligned}
&\text{C1: } P[H_n=k|H_1=l_1,\ldots,H_{n-1}=l_{n-1},H_{n+1}=l_{n+1},\\
&\qquad \ldots,H_N=l_N]=P[H_n=k]\\
&\text{C2: } P[H_n=k|H_1=l_1,\ldots,H_{n-1}=l_{n-1},H_{n+1}=l_{n+1},\\
&\qquad \ldots,H_{N-1}=l_{N-1}]=P[H_n=k]\\
&\qquad\vdots\\
&\text{CN: } P[H_n=k|H_1=l_1]=P[H_n=k]
\end{aligned} \quad (21)$$

We can calculate the conditional probabilities in the left hand side of the conditions; C1, C2, ..., CN in (21) by using a Markov chain. For C1, we can write a state transition probability of going from state $H_n=k$ to $H_n=m$ as $P[H_n=k\rightarrow H_n=m|H_1=l_1,\ldots,H_{n-1}=l_{n-1},H_{n+1}=l_{n+1},\ \ldots,\ H_N=l_N]$, which is equal to $\bar{p}_{n,k}\pi_n\alpha_{n,k}$. *I.e.,* $P[H_n=k\rightarrow H_n=m|H_1=l_1,\ldots,\ H_{n-1}=l_{n-1},H_{n+1}=l_{n+1},\ldots,H_N=l_N]=\bar{p}_{n,k}\pi_n\alpha_{n,k}$. Similarly, if we write the state transition probabilities for the other conditions C2, ..., CN, we have $P[H_n=k\rightarrow H_n=m|H_1=l_1,\ldots,H_{n-1}=l_{n-1},H_{n+1}=l_{n+1},\ldots,H_N=l_N] = P[H_n=k\rightarrow H_n=m|H_1=l_1,\ldots,H_{n-1}=l_{n-1},H_{n+1}=l_{n+1},\ldots,H_{N-1}=l_{N-1}] = \ldots = P[H_n=k\rightarrow H_n=m|H_1=l_1] = P[H_n=k\rightarrow H_n=m] = P[H_n=k\rightarrow H_n=m]=\bar{p}_{n,k}\pi_n\alpha_{n,m}$. Therefore, in all Markov chains we can create for C1, C2, ..., CN, we have the same transition probabilities, so we have $P[H_n=k|H_1=l_1,\ldots,H_{n-1}=l_{n-1},H_{n+1}=l_{n+1},\ldots,H_N=l_N] = P[H_n=k|H_1=l_1,\ldots,H_{n-1}=l_{n-1},H_{n+1}=l_{n+1},\ldots,H_{N-1}=l_{N-1}] = P[H_n=k|H_1=l_1]=P[H_n=k]$. This proves our claim

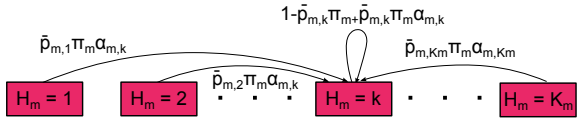

Fig. 10. The state transition diagram for the states $H_m = k$, $\forall k \in \mathcal{K}_m$ and for the mth queue. Note that this state transition diagram only shows a subset of state transitions for clarity.

that $P[H_n = k, H_1 = l_1, \ldots, H_{n-1} = l_{n-1}, H_{n+1} = l_{n+1}, \ldots, H_N = l_N] = P[H_1 = l_1] \ldots P[H_{n-1} = l_{n-1}] P[H_n = k] P[H_{n+1} = l_{n+1}] \ldots P[H_N = l_N]$.

Now that we have shown that $P[H_n = k, H_1 = l_1, \ldots, H_{n-1} = l_{n-1}, H_{n+1} = l_{n+1}, \ldots, H_N = l_N] = P[H_1 = l_1] \ldots P[H_{n-1} = l_{n-1}] P[H_n = k] P[H_{n+1} = l_{n+1}] \ldots P[H_N = l_N]$ holds, (20) is expressed as

$$P[S_1, \ldots, S_N, H_n = k] = \sum_{l_1 \in \mathcal{K}_1} \ldots \sum_{l_{n-1} \in \mathcal{K}_{n-1}} \sum_{l_{n+1} \in \mathcal{K}_{n+1}} \ldots \sum_{l_N \in \mathcal{K}_N} \xi_{1,l_1}(S_1) P[H_1 = l_1] \ldots \xi_{n-1,l_{n-1}}(S_{n-1}) P[H_{n-1} = l_{n-1}] \xi_{n,k}(S_n) P[H_n = k] \xi_{n+1,l_{n+1}}(S_{n+1}) P[H_{n+1} = l_{n+1}] \ldots \xi_{N,l_N}(S_N) P[H_N = l_N], \quad (22)$$

which leads to

$$P[S_1, \ldots, S_N, H_n = k] = \xi_{n,k}(S_n) P[H_n = k] \prod_{m \in \mathcal{N} - \{n\}} \left(\sum_{k \in \mathcal{K}_m} \xi_{m,k}(S_m) P[H_m = k] \right). \quad (23)$$

Now, we should calculate $P[H_m = k]$ in (23). The state transition diagram for the states $H_m = k$, $\forall k \in \mathcal{K}_m$ and for the mth queue is shown in Fig. 10. We can write the global balance equations for the state $H_m = k$ as

$$P[H_m = 1] \bar{p}_{m,1} \pi_m \alpha_{m,k} + \ldots + P[H_m = k][1 - \bar{p}_{m,k} \pi_m + \bar{p}_{m,k} \pi_m \alpha_{m,k}] + \ldots + P[H_m = K_m] \bar{p}_{m,K_m} \pi_m \alpha_{m,k} = P[H_m = k], \quad (24)$$

which is expressed as

$$\pi_m \alpha_{m,k} (\bar{p}_{m,1} P[H_m = 1] + \ldots + \bar{p}_{m,k} P[H_m = k] + \ldots + \bar{p}_{m,K_m} P[H_m = K_m]) = P[H_m = k] \bar{p}_{m,k} \pi_m, \quad (25)$$

which leads to

$$\alpha_{m,k} \sum_{i \in \mathcal{K}_m} \bar{p}_{m,i} P[H_m = i] = P[H_m = k] \bar{p}_{m,k}. \quad (26)$$

Similarly, the global balance equations for state $H_m = l$ leads to

$$\alpha_{m,l} \sum_{i \in \mathcal{K}_m} \bar{p}_{m,i} P[H_m = i] = P[H_m = l] \bar{p}_{m,l}. \quad (27)$$

From (26) and (27), we have

$$\frac{\alpha_{m,k}}{\alpha_{m,l}} = \frac{P[H_m = k] \bar{p}_{m,k}}{P[H_m = l] \bar{p}_{m,l}}. \quad (28)$$

Thus, we have

$$P[H_m = l] = \frac{\alpha_{m,l}}{\bar{p}_{m,l}} \frac{P[H_m = k]}{\alpha_{m,k}} \bar{p}_{m,k}. \quad (29)$$

Since $\sum_{l \in \mathcal{K}_m} P[H_m = l] = 1$ should be satisfied, we have

$$P[H_m = k] = \frac{\lambda_{m,k} / \bar{p}_{m,k}}{\sum_{l \in \mathcal{K}_m} \lambda_{m,l} / \bar{p}_{m,l}}. \quad (30)$$

When (30) is substituted in (23), we have

$$P[S_1, \ldots, S_N, H_n = k] = \xi_{n,k}(S_n) \frac{\lambda_{n,k} / \bar{p}_{n,k}}{\sum_{l \in \mathcal{K}_m} \lambda_{n,l} / \bar{p}_{n,l}} \prod_{m \in \mathcal{N} - \{n\}} \frac{\sum_{k \in \mathcal{K}_m} \xi_{m,k}(S_m) \lambda_{m,k} / \bar{p}_{m,k}}{\sum_{k \in \mathcal{K}_m} \lambda_{m,k} / \bar{p}_{m,k}}. \quad (31)$$

Since $\rho_{m,k}(S_m) = \frac{\xi_{m,k}(S_m)}{\bar{p}_{m,k}}$, we have

$$P[S_1, \ldots, S_N, H_n = k] = \xi_{n,k}(S_n) \frac{\lambda_{n,k} / \bar{p}_{n,k}}{\sum_{l \in \mathcal{K}_m} \lambda_{n,l} / \bar{p}_{n,l}} \prod_{m \in \mathcal{N} - \{n\}} \frac{\sum_{k \in \mathcal{K}_m} \rho_{m,k}(S_m) \lambda_{m,k}}{\sum_{k \in \mathcal{K}_m} \lambda_{m,k} / \bar{p}_{m,k}}. \quad (32)$$

When we substitute (32) into (17), we have (6). This concludes the proof.

Appendix B: Proof of Theorem 3

Let define a Lyapunov function as; $L(\boldsymbol{Q}(t)) = \sum_{n \in \mathcal{N}} Q_n(t)$, and the Lyapunov drift as; $\Delta(\boldsymbol{Q}(t)) = E[L(\boldsymbol{Q}(t+1)) - L(\boldsymbol{Q}(t)) | \boldsymbol{Q}(t)]$, where $\boldsymbol{Q}(t) = \{Q_1(t), \ldots Q_N(t)\}$. Then, the Lyapunov drift is expressed as;

$$\Delta(\boldsymbol{Q}(t)) = E[\sum_{n \in \mathcal{N}} Q_n(t+1)^2 - \sum_{n \in \mathcal{N}} Q_n(t)^2 | \boldsymbol{Q}(t)] \quad (33)$$

Note that we have, from Eq. (1) and the assumption $a_n(t) = \lambda_{n,k}(t) / (\bar{p}_{n,k})^\beta$ that,

$$Q_n(t+1) \leq \max[Q_n(t) - g_n(t), 0] + a_n(t) \sum_{k \in \mathcal{K}_n} (\bar{p}_{n,k})^\beta \quad (34)$$

Using Eq. (34) in Eq. (33), and using the fact that $(\max(Q - b, 0) + A)^2 \leq Q^2 + A^2 + b^2 + 2Q(A - b)$, we have

$$\Delta(\boldsymbol{Q}(t)) \leq E[\sum_{n \in \mathcal{N}} \{Q_n(t)^2 + (a_n(t) \sum_{k \in \mathcal{K}_n} (\bar{p}_{n,k})^\beta)^2 + (g_n(t))^2 + 2Q_n(t)(a_n(t) \sum_{k \in \mathcal{K}_n} (\bar{p}_{n,k})^\beta - g_n(t))\} - \sum_{n \in \mathcal{N}} Q_n(t)^2 | \boldsymbol{Q}(t)] \quad (35)$$

which is expressed as

$$\frac{\Delta(\boldsymbol{Q}(t))}{2 \sum_{k \in \mathcal{K}_n} (\bar{p}_{n,k})^\beta} \leq E[\sum_{n \in \mathcal{N}} \{\frac{(a_n(t))^2}{2} \sum_{k \in \mathcal{K}_n} (\bar{p}_{n,k})^\beta + \frac{(g_n(t))^2}{2 \sum_{k \in \mathcal{K}_n} (\bar{p}_{n,k})^\beta} + Q_n(t) a_n(t) - \frac{Q_n(t) g_n(t)}{\sum_{k \in \mathcal{K}_n} (\bar{p}_{n,k})^\beta}\} | \boldsymbol{Q}(t)] \quad (36)$$

There always exist a finite and positive B satisfying; $B \geq E\big[\sum_{n\in\mathcal{N}}\big\{\frac{(a_n(t))^2}{2}\sum_{k\in\mathcal{K}_n}(\bar{p}_{n,k})^\beta + \frac{(g_n(t))^2}{2\sum_{k\in\mathcal{K}_n}(\bar{p}_{n,k})^\beta}\big\}\big]$. Thus, Eq. (36) is expressed as;

$$\frac{\Delta(\boldsymbol{Q}(t))}{2\sum_{k\in\mathcal{K}_n}(\bar{p}_{n,k})^\beta} \leq B + E\big[\sum_{n\in\mathcal{N}} Q_n(t)\big(a_n(t) - \frac{g_n(t)}{\sum_{k\in\mathcal{K}_n}(\bar{p}_{n,k})^\beta}\big)|\boldsymbol{Q}(t)\big] \tag{37}$$

Note that if the flow arrival rates $\lambda_{n,k}(t) = a_n(t)(\bar{p}_{n,k})^\beta$ are inside the capacity region $\tilde{\Lambda}$, then the minimizing the right hand side of the drift inequality in Eq. (37) corresponds to the scheduling part of qFC in Eq. (14).

Now, let us consider again the stability region constraint in Eq. (17), which is $\lambda_{n,k} \leq \sum_{(S_1,\ldots,S_N)\in\mathcal{S}} P[S_1,\ldots,S_N, H_n = k]1_{[S_n]}\tau_n(S_1,\ldots,S_N), \forall n \in \mathcal{N}, k \in \mathcal{K}_n$, and expressed as;

$$\sum_{k\in\mathcal{K}_n}\lambda_{n,k} \leq \sum_{(S_1\ldots S_N)\in\mathcal{S}}\big(\sum_{k\in\mathcal{K}_n} P[S_1\ldots S_N, H_n = k]\big)1_{[S_n]}\tau_n(S_1\ldots S_N) \tag{38}$$

which is equal to

$$\sum_{k\in\mathcal{K}_n}\lambda_{n,k} \leq \sum_{(S_1\ldots S_N)\in\mathcal{S}} P[S_1\ldots S_N]1_{[S_n]}\tau_n(S_1\ldots S_N) \tag{39}$$

Since $\lambda_{n,k} = a_n(\bar{p}_{n,k})^\beta$, we have

$$\sum_{k\in\mathcal{K}_n} a_n(\bar{p}_{n,k})^\beta \leq \sum_{(S_1\ldots S_N)\in\mathcal{S}} P[S_1\ldots S_N]1_{[S_n]}\tau_n(S_1\ldots S_N) \tag{40}$$

$$a_n\sum_{k\in\mathcal{K}_n}(\bar{p}_{n,k})^\beta \leq \sum_{(S_1\ldots S_N)\in\mathcal{S}} P[S_1\ldots S_N]1_{[S_n]}\tau_n(S_1\ldots S_N) \tag{41}$$

$$a_n \leq \sum_{(S_1\ldots S_N)\in\mathcal{S}} P[S_1\ldots S_N]\frac{1_{[S_n]}\tau_n(S_1\ldots S_N)}{\sum_{k\in\mathcal{K}_n}(\bar{p}_{n,k})^\beta} \tag{42}$$

Let $g_n = 1_{[S_n]}\tau_n(S_1\ldots S_N)$. Then, Eq. (42) is expressed as;

$$a_n \leq \sum_{(S_1\ldots S_N)\in\mathcal{S}} P[S_1\ldots S_N]\frac{g_n}{\sum_{k\in\mathcal{K}_n}(\bar{p}_{n,k})^\beta} \tag{43}$$

There exists a small positive value ϵ satisfying

$$a_n + \epsilon \leq \sum_{(S_1\ldots S_N)\in\mathcal{S}} P[S_1\ldots S_N]\frac{g_n}{\sum_{k\in\mathcal{K}_n}(\bar{p}_{n,k})^\beta} \tag{44}$$

Thus, we can find a randomized policy satisfying

$$E\big[\overset{*}{a}_n(t) - \frac{\overset{*}{g}_n(t)}{\sum_{k\in\mathcal{K}_n}(\bar{p}_{n,k})^\beta}\big] \leq -\epsilon \tag{45}$$

Now, let us consider Eq. (37) again, which is expressed as;

$$\frac{\Delta(\boldsymbol{Q}(t))}{2\sum_{k\in\mathcal{K}_n}(\bar{p}_{n,k})^\beta} \leq B + \sum_{n\in\mathcal{N}} Q_n(t)E\big[a_n(t) - \frac{g_n(t)}{\sum_{k\in\mathcal{K}_n}(\bar{p}_{n,k})^\beta}|\boldsymbol{Q}(t)\big] \tag{46}$$

We minimize the right hand side of Eq. (37), so the following inequality satisfies;

$$E\big[a_n(t) - \frac{g_n(t)}{\sum_{k\in\mathcal{K}_n}(\bar{p}_{n,k})^\beta}|\boldsymbol{Q}(t)\big] \leq E\big[\overset{*}{a}_n(t) - \frac{\overset{*}{g}_n(t)}{\sum_{k\in\mathcal{K}_n}(\bar{p}_{n,k})^\beta}|\boldsymbol{Q}(t)\big] \tag{47}$$

where $\overset{*}{a}_n(t)$ and $\overset{*}{g}_n(t)$ are the solutions of a randomized policy. Incorporating Eq. (45) in Eq. (47), we have

$$\frac{\Delta(\boldsymbol{Q}(t))}{2\sum_{k\in\mathcal{K}_n}(\bar{p}_{n,k})^\beta} \leq B - \epsilon\sum_{n\in\mathcal{N}} Q_n(t) \tag{48}$$

The time average of Eq. (48) leads to

$$\limsup_{t\to\infty}\frac{1}{t}\sum_{\tau=0}^{t-1}\frac{\Delta(\boldsymbol{Q}(\tau))}{2\sum_{k\in\mathcal{K}_n}(\bar{p}_{n,k})^\beta} \leq \limsup_{t\to\infty}\frac{1}{t}\sum_{\tau=0}^{t-1}\big[B - \epsilon\sum_{n\in\mathcal{N}} Q_n(\tau)\big] \tag{49}$$

$$\limsup_{t\to\infty}\frac{1}{t}\sum_{\tau=0}^{t-1}\big(\sum_{n\in\mathcal{N}} Q_n(\tau)\big) \leq \frac{B}{\epsilon} \tag{50}$$

This concludes that the time average of the queues are bounded if the arrival rates are inside the capacity region $\tilde{\Lambda}$.

Now, let us focus on the original claim of Theorem 2. Let us consider a drift+penalty function as;

$$\frac{\Delta(\boldsymbol{Q}(t))}{2\sum_{k\in\mathcal{K}_n}(\bar{p}_{n,k})^\beta} - \sum_{n\in\mathcal{N}}\sum_{k\in\mathcal{K}_n} ME[U_{n,k}(\lambda_{n,k}(t))|\boldsymbol{Q}(t)] \leq B + E\big[\sum_{n\in\mathcal{N}} Q_n(t)\big(a_n(t) - \frac{g_n(t)}{\sum_{k\in\mathcal{K}_n}(\bar{p}_{n,k})^\beta}\big)|\boldsymbol{Q}(t)\big] - \sum_{n\in\mathcal{N}}\sum_{k\in\mathcal{K}_n} ME[U_{n,k}(\lambda_{n,k}(t))|\boldsymbol{Q}(t)] \tag{51}$$

Since we set $\lambda_{n,k}(t) = a_n(t)(\bar{p}_{n,k})^\beta$, we have

$$\frac{\Delta(\boldsymbol{Q}(t))}{2\sum_{k\in\mathcal{K}_n}(\bar{p}_{n,k})^\beta} - \sum_{n\in\mathcal{N}}\sum_{k\in\mathcal{K}_n} ME[U_{n,k}(a_n(t)(\bar{p}_{n,k})^\beta)|\boldsymbol{Q}(t)] \leq B + \sum_{n\in\mathcal{N}} E\big[Q_n(t)\big(a_n(t) - \frac{g_n(t)}{\sum_{k\in\mathcal{K}_n}(\bar{p}_{n,k})^\beta}\big)|\boldsymbol{Q}(t)\big] - \sum_{n\in\mathcal{N}}\sum_{k\in\mathcal{K}_n} ME[U_{n,k}(a_n(t)(\bar{p}_{n,k})^\beta)|\boldsymbol{Q}(t)] \tag{52}$$

Note that minimizing the right hand side of Eq. (52) corresponds to the flow control and scheduling algorithms of qFC in Eq. (13) and Eq. (14), respectively. Since there exists a randomized policy satisfying Eq. (45), Eq. (52) is expressed as

$$\frac{\Delta(\boldsymbol{Q}(t))}{2\sum_{k\in\mathcal{K}_n}(\bar{p}_{n,k})^\beta} - \sum_{n\in\mathcal{N}}\sum_{k\in\mathcal{K}_n} ME[U_{n,k}(a_n(t)(\bar{p}_{n,k})^\beta)|\boldsymbol{Q}(t)] \leq B - \epsilon\sum_{n\in\mathcal{N}} Q_n(t) - \sum_{n\in\mathcal{N}}\sum_{k\in\mathcal{K}_n} MU_{n,k}(A_n(\bar{p}_{n,k})^\beta + \delta) \tag{53}$$

where $\sum_{n\in\mathcal{N}}\sum_{k\in\mathcal{K}_n} U_{n,k}(A_n(\bar{p}_{n,k})^\beta+\delta)$ is the maximum time average of the sum utility function that can be achieved by any control policy that stabilizes the system. Then, the time average of Eq. (53) becomes

$$\limsup_{t\to\infty}\frac{1}{t}\sum_{\tau=0}^{t-1}\Bigg\{\frac{\Delta(Q(\tau))}{2\sum_{k\in\mathcal{K}_n}(\bar{p}_{n,k})^\beta}- \sum_{n\in\mathcal{N}}\sum_{k\in\mathcal{K}_n} ME[U_{n,k}(a_n(\tau)(\bar{p}_{n,k})^\beta)|\boldsymbol{Q}(t)]\Bigg\}\leq \limsup_{t\to\infty}\frac{1}{t}\sum_{\tau=0}^{t-1}\Bigg\{B-\epsilon\sum_{n\in\mathcal{N}}Q_n(\tau)- \sum_{n\in\mathcal{N}}\sum_{k\in\mathcal{K}_n} MU_{n,k}(A_n(\bar{p}_{n,k})^\beta+\delta)\Bigg\} \quad (54)$$

Now, let us first consider the stability of the queues. If both sides of Eq. (54) is divided by ϵ and the terms are arranged, we have

$$\limsup_{t\to\infty}\frac{1}{t}\sum_{\tau=0}^{t-1}\Big\{\sum_{n\in\mathcal{N}}Q_n(\tau)\Big\}\leq\frac{B}{\epsilon}+\limsup_{t\to\infty}\frac{1}{t}\sum_{\tau=0}^{t-1}\Big\{\sum_{n\in\mathcal{N}}\sum_{k\in\mathcal{K}_n} \frac{M}{\epsilon}E[U_{n,k}(a_n(\tau)(\bar{p}_{n,k})^\beta)]\Big\}-\sum_{k\in\mathcal{N}}\sum_{k\in\mathcal{K}_n}\frac{M}{\epsilon}U_{n,k}(A_n(\bar{p}_{n,k})^\beta+\delta) \quad (55)$$

Since the right hand side is a positive finite value, this concludes that the time averages of the total queue sizes are bounded.

Now, let us consider the optimality. If both sides of Eq. (54) are divided by M, we have

$$-\limsup_{t\to\infty}\frac{1}{t}\sum_{\tau=0}^{t-1}\sum_{n\in\mathcal{N}}\sum_{k\in\mathcal{K}_n}E[U_{n,k}(a_n(\tau)(\bar{p}_{n,k})^\beta)]\leq \limsup_{t\to\infty}\frac{1}{t}\sum_{\tau=0}^{t-1}\Big\{\frac{B}{M}-\frac{\epsilon}{M}\sum_{n\in\mathcal{N}}Q_n(\tau)- \sum_{n\in\mathcal{N}}\sum_{k\in\mathcal{K}_n}U_{n,k}(A_n(\bar{p}_{n,k})^\beta+\delta)\Big\} \quad (56)$$

By arranging the terms, we have

$$\limsup_{t\to\infty}\frac{1}{t}\sum_{\tau=0}^{t-1}\sum_{n\in\mathcal{N}}\sum_{k\in\mathcal{K}_n}E[U_{n,k}(a_n(\tau)(\bar{p}_{n,k})^\beta)]\geq \limsup_{t\to\infty}\frac{1}{t}\sum_{\tau=0}^{t-1}\Big\{\sum_{n\in\mathcal{N}}\sum_{k\in\mathcal{K}_n}U_{n,k}(A_n(\bar{p}_{n,k})^\beta+\delta)-\frac{B}{M} +\frac{\epsilon}{M}\sum_{n\in\mathcal{N}}Q_n(\tau)\Big\} \quad (57)$$

Since $\frac{\epsilon}{M}\sum_{n\in\mathcal{N}}Q_n(\tau)$ is positive for any τ, we have

$$\limsup_{t\to\infty}\frac{1}{t}\sum_{\tau=0}^{t-1}\sum_{n\in\mathcal{N}}\sum_{k\in\mathcal{K}_n}E[U_{n,k}(a_n(\tau)(\bar{p}_{n,k})^\beta)]\geq \limsup_{t\to\infty}\frac{1}{t}\sum_{\tau=0}^{t-1}\Big\{\sum_{n\in\mathcal{N}}\sum_{k\in\mathcal{K}_n}U_{n,k}(A_n(\bar{p}_{n,k})^\beta+\delta)-\frac{B}{M}\Big\} \quad (58)$$

which leads to

$$\limsup_{t\to\infty}\frac{1}{t}\sum_{\tau=0}^{t-1}\sum_{n\in\mathcal{N}}\sum_{k\in\mathcal{K}_n}E[U_{n,k}(a_n(\tau)(\bar{p}_{n,k})^\beta)]\geq \sum_{n\in\mathcal{N}}\sum_{k\in\mathcal{K}_n}U_{n,k}(A_n(\bar{p}_{n,k})^\beta+\delta)-\frac{B}{M} \quad (59)$$

This proves that the admitted flow rates converge to the utility optimal operating point with increasing M. This concludes the proof.